(Received 23 June 2025, Accepted 27 August 2025, Scheduled 4 September 2025)

A Substrate Integrated Half-Coaxial Line (SIHCL) and Its Application in Low-Pass Filter with Low Crosstalk

Yu-Fan Chi, Yang-Qing Xu, Qing-Cheng Zhang, Wen-Xuan Shen, Yan He, Yan-Yan Kong, and Lin Li*

Zhejiang Sci-Tech University, China

ABSTRACT: To achieve compact size and high electromagnetic shielding performance in RF systems, a substrate integrated half-coaxial line (SIHCL) structure is proposed. A new approximate synthesis method for the SIHCL is proposed using the equivalent capacitor. Subsequently, two fifth-order Chebyshev low-pass filters (LPFs) with a 0.1 dB ripple factor were designed and fabricated: the first implemented in the SIHCL structure and the second in microstrip technology. A comparison of the measured S-parameters between these two low-pass filters demonstrates that both near-end and far-end crosstalk is suppressed for the proposed SIHCL LPF, which is significant for high-speed and high-density integrated systems.

1. INTRODUCTION

With the growth of wireless communication, radio frequency (RF) systems are evolving toward increasingly dense configurations. Therefore, electromagnetic compatibility (EMC) in a miniaturized electrical system with multiple components considerations becomes essential to ensure reliable functionality of all systems [1, 2]. EMC has become a pivotal challenge for unlocking the full potential of the internet of everything (IOE) and future joint-communication and sensing (JCAS) 6G applications [3].

Self-shielding transmission lines exhibit excellent electromagnetic compatibility (EMC) performance, which helps compress component spacing and increase circuit integration density. For one thing, they prevent electromagnetic interference from the external components; for another, they also suppress the radiation of internal signals to the external environment [4]. As a result, the employment of self-shielding transmission lines helps to compress component spacing and leads to a high-density integrated circuit system.

Traditional coaxial lines and rectangular waveguides (RWGs) yield most favorable shielding properties [5] but are difficult to integrate with standard printed circuit board (PCB) manufacturing. Substrate integrated waveguide (SIW) offers an interesting solution, but suffers from relatively large dimensions, making them unsuitable for high-density system integration [6–8].

Substrate integrated coaxial line (SICL), first introduced in [9], is a three-conductor transmission line that implements the rectangular coaxial line in planar substrates. The electromagnetic field in SICL resembles the transverse electromagnetic (TEM) mode propagation in conventional coaxial line. The middle conducting plate is sandwiched between the top and bottom plates, encapsulating between two rows of vias on either side that provides it effective shielding. Recently, several research works on antenna and circuit design in the novel SICL technology have been proposed [10–13]. However, SICL's stacked dual-dielectric-substrate configuration inevitably increases its overall dimensions compared to compact planar transmission lines such as microstrip. This enlarged footprint fundamentally limits the applicability of SICLs in high-density integrated circuits. Furthermore, the dual-substrate architecture necessitates higher material consumption, more complex fabrication processes, and increased production costs than single-substrate lines like microstrip. Additionally, achieving precise alignment of interlayer metallized vias while maintaining uniform adhesive layers presents significant fabrication challenges.

To fully exploit the self-shielding properties of substrate integrated coaxial transmission lines while overcoming their limitations in bulkiness and cost, this paper proposes a novel substrate integrated half-coaxial line (SIHCL) structure, which comprises a printed coaxial topology laterally shielded by metallized vias. Its structure consists of a central conductor strip patterned on the dielectric substrate surface, sandwiched between a continuous ground plane beneath and an air cladding above. Due to the dielectric inhomogeneity of this configuration, the electric fields cannot be entirely confined within a uniform medium, leading to partial field penetration into the air region. This field distribution in heterogeneous dielectrics generates non-negligible longitudinal field components, establishing quasi-TEM mode propagation as the dominant mechanism — analogous to conventional microstrip lines. Both structures deviate from ideal TEM mode conditions which require zero longitudinal fields due to dielectric non-uniformity. Nevertheless, transverse field components remain predominant, allowing TEM-mode approximation for analysis and design pur-

* Corresponding author: Lin Li (lilin_door@hotmail.com).

poses [5]. A new synthesis method based on equivalent capacitance theory of transmission is introduced, and its accuracy is validated through comparison with electromagnetic simulation results. Two fifth-order Chebyshev low-pass filters with a cutoff frequency of 0.85 GHz and a ripple factor of 0.1 dB were designed: the first implemented using the SIHCL structure and the second based on a conventional microstrip line configuration. Comparative test results demonstrate that the SIHCL low-pass filter not only exhibits excellent low-pass filtering characteristics but also demonstrates superior self-shielding properties, effectively suppressing crosstalk with adjacent microstrip lines.

2. SIHCL AND ITS SYNTHESIS METHOD

Figure 1 depicts the geometry structure of the proposed SIHCL. The structure consists of a top conductor strip, a middle dielectric layer, a bottom ground, and two symmetrical rows of metallic via-holes. The conductor strip with a width of $w1$ is on the top of the FR4 substrate with a relative permittivity of 4.4, a thickness of $h = 0.8$ mm. g is the distance between the inner conductor strip and the via-holes. The via-holes have a diameter of 1 mm and a period of 2 mm.

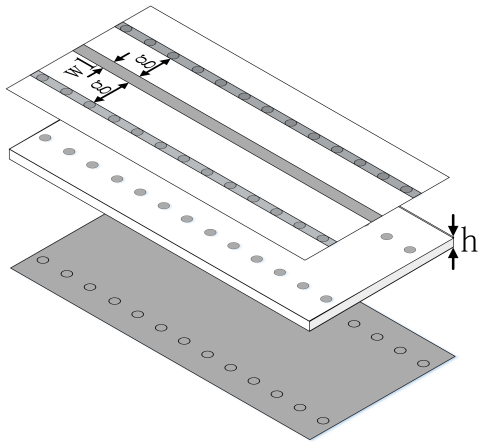

FIGURE 1. The geometry structure of the proposed SIHCL.

To synthesize the proposed SIHCL, a new method based on the equivalent capacitance of the transmission lines is developed when the vias on both sides are equivalently treated as metal walls. Figure 2 illustrates the equivalent capacitance distribution across the SIHCL cross-section. C_1 represents the inter-plate capacitance between the conductive strip and adjacent metal walls. C_2 denotes the inter-plate capacitance between the conductive strip and bottom ground plane. C_{f1} and C_{f2} characterize the corner capacitance arising between the conductive strip and adjacent walls and bottom metal ground, respectively.

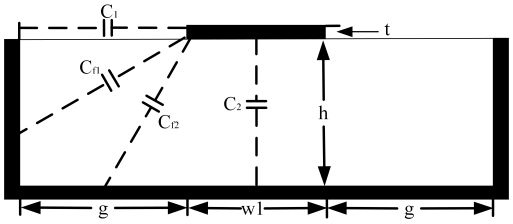

FIGURE 2. Capacitance distribution of the SIHCL.

Based on the equivalent capacitance formula for SICL described in [14], the equivalent capacitance of the SIHCL can be expressed as:

$$C_1 = \frac{\varepsilon_1 t}{g} \tag{1}$$

$$C_2 = \frac{\varepsilon_2 w}{h} \tag{2}$$

$$C_{f1} = \frac{\varepsilon_1}{\pi}\left(\log\frac{g^2+h^2}{4h^2} + 2\frac{h}{g}\arctan\frac{g}{h}\right) \tag{3}$$

$$C_{f2} = \frac{\varepsilon_1}{\pi}\left(\log\frac{g^2+h^2}{4g^2} + 2\frac{g}{h}\arctan\frac{h}{g}\right) \tag{4}$$

ε_1 denotes the dielectric constant calculated using the permittivity, ε_2 the dielectric constant calculated using the permittivity, and t the thickness of the inner conductor, where the thickness of the inner conductor is $t = 0.018$ mm. The expression for ε_1 is given by [15]:

If $W/h \leq 1$:

$$\varepsilon_1 = \frac{\varepsilon_r+1}{2} + \frac{\varepsilon_r-1}{2}\left\{\left[1+12\frac{h}{W}\right]^{-\frac{1}{2}} + 0.04\left[1-\frac{W}{h}\right]^2\right\} \tag{5}$$

If $W/h \geq 1$:

$$\varepsilon_1 = \frac{\varepsilon_r+1}{2} + \frac{\varepsilon_r-1}{2}\left[1+12\frac{h}{W}\right]^{-\frac{1}{2}} \tag{6}$$

Since the SIHCL structure is derived by symmetrically halving the thickness of the SICL structure, the total capacitance of the SIHCL can be modeled as:

$$C = 2(C_1 + C_{f1} + C_{f2}) + C_2 \tag{7}$$

Thus, the characteristic impedance of the SIHCL can be computed as:

$$Z_{\text{SIHCL}} = \frac{1}{v_p C} \tag{8}$$

v_p denotes the phase velocity of the electromagnetic wave. This approach establishes the relationship between the physical dimensions of the SIHCL and its characteristic impedance. Based on the derived methods, under a fixed pitch between dual-row metallized vias, Figure 3 illustrates the variation in characteristic impedance with respect to the center conductor width $w1$ and conductor-to-via clearance.

The High Frequency Structure Simulator (HFSS) simulated $|S_{11}|$ of the proposed SIHCLs with different $w1$ is also shown in Figure 3. As displayed in Figure 3, the calculated and simulated $|S_{11}|$ curves in the three figures show excellent agreement, which validates the effectiveness of the proposed method.

TABLE 1. Dimension parameters of the two low-pass filters designed in this paper.

Element name	Element values (mm)	Element name	Element values (mm)
W_{s1}	6.6	W_{m1}	6.6
W_{s2}	0.2	W_{m2}	0.2
W_{s6}	8.1	L_{m1}	10.45
L_{s1}	10.15	L_{m2}	17.78
L_{s2}	17.36	L_{m3}	18.03
L_{s3}	17.11	h	0.8

Unit: $W_{s1} = W_{s3} = W_{s5}$; $W_{s2} = W_{s4}$; $L_{s1} = L_{s5}$; $L_{s2} = L_{s4}$; $W_{m1} = W_{m3} = W_{m5}$; $W_{m2} = W_{m4}$; $L_{m1} = L_{m5}$; $L_{m2} = L_{m4}$.

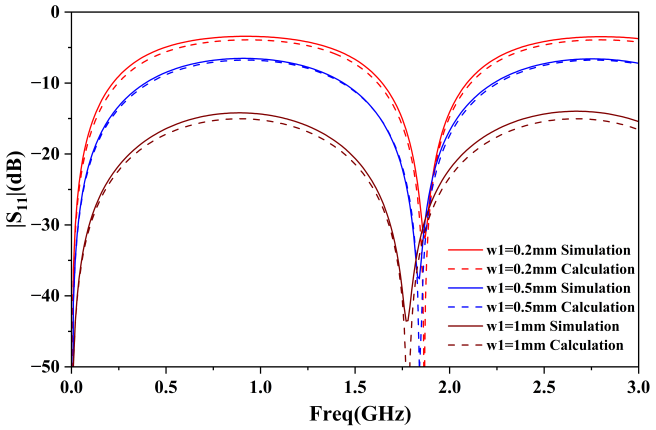

FIGURE 3. Comparison of the calculated and simulated $|S_{11}|$ for SIHCL with different $w1$.

3. FABRICATION AND TEST OF SIHCL

Considering the widespread use of microstrip low-pass filters (LPFs) in RF systems [16–19], LPFs are used to behave as the victim component. The crosstalk between the victim and aggressor components is utilized to evaluate the electromagnetic shielding performance of the SIHCL configuration. For comparative purposes, low-pass filters were designed not only with SIHCL but also with microstrip lines. Both fifth-order LPFs have a ripple factor of 0.1 dB and a cutoff frequency f_c of 0.85 GHz. If both the source and load impedance are set to $Z_0 = 50\,\Omega$, the corresponding LC circuit prototype is depicted in Figure 4. The component values are as follows: $C1 = C5 = 4.2946$ pF, $L2 = L4 = 12.8373$ nH, $C3 = 7.3960$ pF. By using high-impedance lines to realize the inductors and low-impedance lines to realize the capacitors, two LPFs are obtained as illustrated in Figure 5.

The physical lengths of the high-impedance lines and low-impedance lines are calculated using the following formulas [20]:

$$l_L = \frac{\lambda_{gL}}{2\pi}\sin^{-1}\left(\frac{2\pi f_c L}{Z_{OL}}\right) \tag{9}$$

$$l_C = \frac{\lambda_{gc}}{2\pi}\sin^{-1}\left(2\pi f_c C Z_{OC}\right) \tag{10}$$

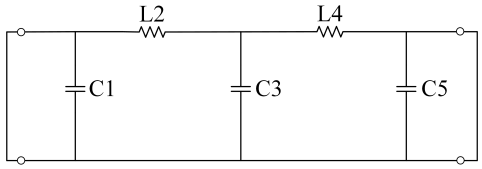

FIGURE 4. Schematic of the prototype ideal LC circuit.

where l_L and l_C represent the lengths of high-characteristic-impedance transmission lines and low-characteristic-impedance transmission lines, respectively; λ_{gL} and λ_{gc} represent the wavelengths of the high-characteristic-impedance and low-characteristic-impedance transmission lines, respectively.

In this design, the two filters have identical widths for their inductive and capacitive sections. The optimal dimensional parameters of the two low-pass filters are listed in Table 1 which defines the structural parameters of both filters. For the SIHCL low-pass filter, W_{s1}–W_{s5} denote the widths of feed line sections; L_{s1}–L_{s5} denote the corresponding section lengths; W_{s6} denotes the pitch between two rows of metallized vias; for the microstrip low-pass filter, W_{m1}–W_{m5} represent the widths of feed line; L_{m1}–L_{m5} represent the lengths of feed lines; h represents the dielectric substrate thickness for both configurations.

When LPFs are designed, microstrip lines with the characteristic impedance of $50\,\Omega$ are introduced to behave as the aggressor components. The distance between the aggressor line and victim LPF is set to 1.45 mm. Furthermore, the crosstalk between the two components can be divided into near-end crosstalk (NEXT) and far-end crosstalk (FEXT), with reference to the end of the line adjacent to the end of the generator circuit. Photographs of the two LPFs with the aggressor lines are shown in Figure 6.

The measured transmission and reflection coefficients of both filters are shown in Figure 7(a). The SIHCL low-pass filter has a 3 dB cutoff frequency f_c at 0.9 GHz, with a minimum insertion loss (IL) of less than 0.2 dB and a minimum return loss (RL) of 10.9 dB in the passband. The microstrip low-pass filter also has a 3 dB cutoff frequency f_c at 0.9 GHz, with a minimum IL of less than 0.13 dB and a minimum RL of 11.7 dB in the passband. Obviously, the two filters have similar signal transmission performances.

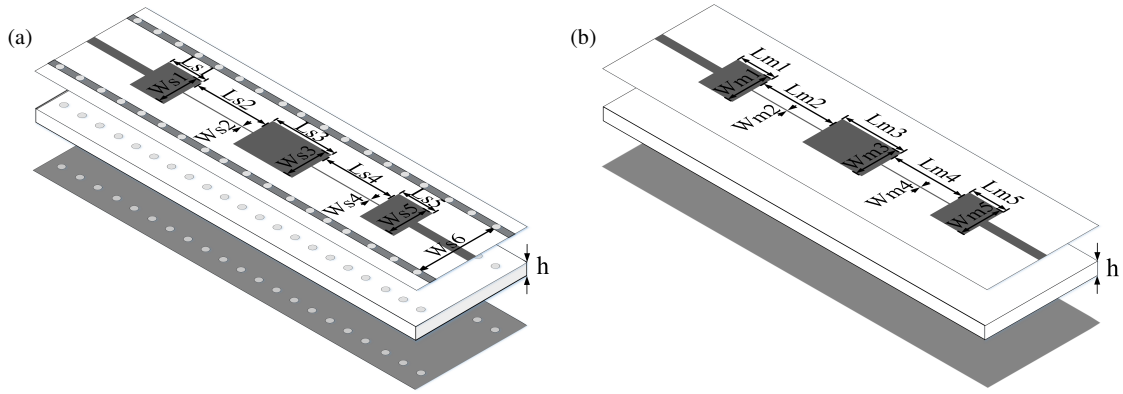

FIGURE 5. Structures of the two low-pass filters designed in this paper. (a) Structure of the low-pass filter based on the SIHCL structure. (b) Structure of the low-pass filter based on the microstrip structure.

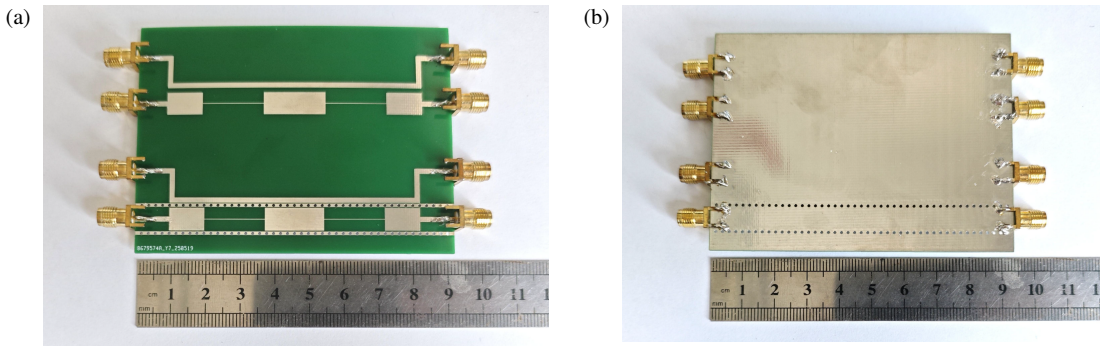

FIGURE 6. Diagrams of SIHCL low-pass filters and microstrip low-pass filter prototypes. (a) Top view of two low-pass filter prototypes. (b) Bottom view of two low-pass filter prototypes.

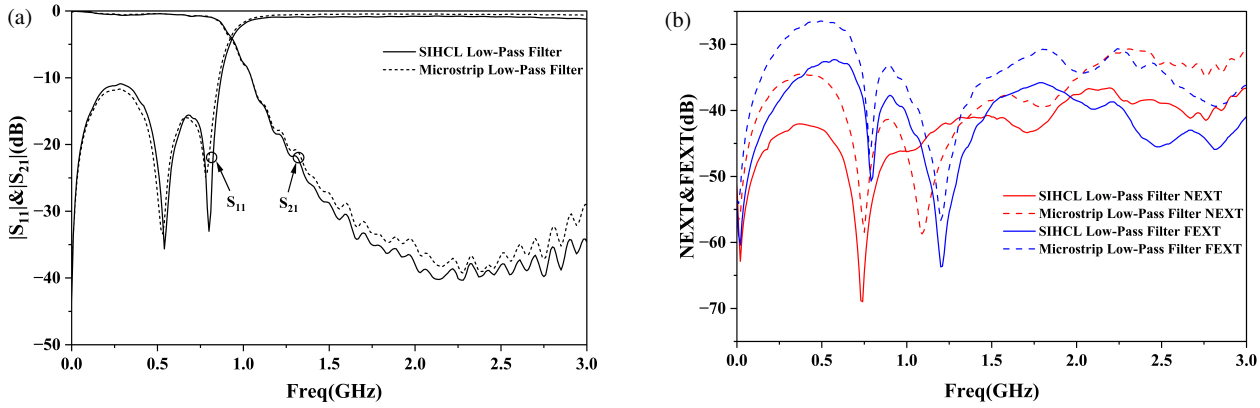

FIGURE 7. Simulated performance comparison between the SIHCL and microstrip low-pass filters. (a) Comparative figures of $|S_{11}|$ and $|S_{21}|$ for two low-pass filters. (b) Comparative figures of NEXT and FEXT for two low-pass filters.

The self-shielded effect based on the proposed SIHCL should also be verified. In order to analyze the crosstalk, the aggressor line is excited at port 1. The measured near-end ($|S_{31}|$) and far-end crosstalk ($|S_{41}|$) of the two LPFs are compared in Figure 7(b). It can be clearly observed that the crosstalk from Figure 7(b) for the SIHCL LPF is lower than that for the microstrip LPF in almost the whole frequency. At 0.39 GHz, the near-end crosstalk of the SIHCL low-pass filter is -42.1 dB, representing a maximum improvement of 7.6 dB over the microstrip low-pass filter's -34.5 dB. At 0.85 GHz, the far-end crosstalk of the SIHCL low-pass filter is -39.8 dB, demonstrating a maximum 5.4 dB improvement over the microstrip low-pass filter's -34.4 dB.

In summary, the SIHCL exhibits good EMC performance, which helps to reduce the distance of the adjacent components. Thus, the system with more compact size can be realized.

Table 2 presents a performance comparison between the SIHCL low-pass filter and some reported high-performance

TABLE 2. Comparison of the SIHCL low-pass filter with other works.

Refs.	f_c (GHz)	IL (dB)	RL (dB)	NCS (λ_g^2)
[12]	4.3	0.5	18.8	0.014
[13]	2.4	2.4	20	0.011
[16]	1.3	0.3	8	0.0107
[17]	2.11	0.7	13	0.032
[18]	1.26	0.3	10	0.0053
[19]	2.56	0.7	8	0.612
This work	0.9	0.3	11.2	0.023

LPFs [12, 13, 16–19]. There are some important parameters of LPF: IL is the minimum insertion loss; RL is the minimum return loss in the passband; NSC is the circuit size normalized by λ_g, where λ_g is the microstrip line guided wavelength at f_c.

Figure 7(a) illustrates that SIHCL low-pass filter has a 3 dB cutoff frequency f_c at 0.9 GHz. The minimum insertion loss (IL) is less than 0.3 dB, and the minimum return loss (RL) in the passband is 11.2 dB. The size of the SIHCL low-pass filter is 92 mm $\times$ 9.1 mm, corresponding to $0.48\lambda_g \times 0.048\lambda_g$.

As demonstrated in Table 2, the proposed SIHCL low-pass filter achieves competitive performance in core metrics including insertion loss (0.3 dB) and return loss (11.2 dB). Its innovative structure provides superior electromagnetic shielding compared to traditional microstrip-based low-pass filters, while also maintaining a streamlined fabrication process and a compact footprint relative to SICL filters.

4. CONCLUSION

Substrate integrated half-coaxial lines (SIHCLs) are presented. The proposed SIHCLs exhibit excellent self-shielded properties, a simple structure, and low cost. Using transmission line theory, a new synthesis method for SIHCL has been proposed, providing the relationship between dimensions and characteristics impedance. Finally, the validity and usefulness of the proposed SIHCL and corresponding method have been demonstrated for an LPF design with low crosstalk.

REFERENCES

[1] Takahashi, K., Y. Murata, Y. Tsubaki, T. Fujiwara, H. Maniwa, and N. Uehara, "Mechanism of near-field coupling between noise source and EMI filter in power electronic converter and its required shielding," *IEEE Transactions on Electromagnetic Compatibility*, Vol. 61, No. 5, 1663–1672, 2019.

[2] Tang, M., J. Lu, J. Mao, and L. Jiang, "A systematic electromagnetic-circuit method for EMI analysis of coupled interconnects on dispersive dielectrics," *IEEE Transactions on Microwave Theory and Techniques*, Vol. 61, No. 1, 1–13, 2013.

[3] Liu, F., C. Masouros, A. P. Petropulu, H. Griffiths, and L. Hanzo, "Joint radar and communication design: Applications, state-of-the-art, and the road ahead," *IEEE Transactions on Communications*, Vol. 68, No. 6, 3834–3862, 2020.

[4] Pozar, D. M., *Microwave Engineering*, Wiley-Interscience, New York, 2005.

[5] Wu, K., M. Bozzi, and N. J. G. Fonseca, "Substrate integrated transmission lines: Review and applications," *IEEE Journal of Microwaves*, Vol. 1, No. 1, 345–363, 2021.

[6] Al-Sayadi, A., H. Vettikalladi, and M. A. S. Alkanhal, "Millimeter wave antenna based on SIW technology for WLAN/WPAN 5G networks at 60 GHz," in *2017 International Conference on Electrical and Computing Technologies and Applications (ICECTA)*, 1–4, Ras Al Khaimah, United Arab Emirates, 2017.

[7] Wang, N.-N., B.-X. Zhao, T.-Y. Du, and J.-X. Liu, "A W-band directional radiation antenna loading dielectric sheet based on SIW technology," in *2017 International Symposium on Antennas and Propagation (ISAP)*, 1–2, Phuket, Thailand, 2017.

[8] Hou, Y., Y. Zhang, and J. Mao, "A differential dual-polarized laminated resonator antenna with backed SIW cavity excitation," in *2021 IEEE International Symposium on Antennas and Propagation and USNC-URSI Radio Science Meeting (APS/URSI)*, 1675–1676, Singapore, 2021.

[9] Gatti, F., M. Bozzi, L. Perregrini, K. Wu, and R. G. Bosisio, "A novel substrate integrated coaxial line (SICL) for wide-band applications," in *2006 European Microwave Conference*, 1614–1617, Manchester, UK, 2006.

[10] Van Messem, L., A. Moerman, O. Caytan, H. Rogier, and S. Lemey, "Compact self-shielding components for beamforming networks implemented in substrate integrated coaxial line technology," *IEEE Transactions on Components, Packaging and Manufacturing Technology*, Vol. 15, No. 1, 15–21, 2025.

[11] Krishna, I. S. and S. Mukherjee, "Design of wideband microstrip to SICL transition for millimeter-wave applications," *IEEE Access*, Vol. 8, 4250–4254, 2020.

[12] Yang, D. and Y. Dong, "Miniaturized integrated bandstop filter with high in-band performance based on substrate integrated coaxial line," *IEEE Electron Device Letters*, Vol. 46, No. 6, 1003–1006, 2025.

[13] Chu, P., W. Hong, L. Dai, H. Tang, Z. Hao, J. Chen, and K. Wu, "Wide stopband bandpass filter implemented with spur stepped impedance resonator and substrate integrated coaxial line technology," *IEEE Microwave and Wireless Components Letters*, Vol. 24, No. 4, 218–220, 2014.

[14] Chen, T.-S., "Determination of the capacitance, inductance, and characteristic impedance of rectangular lines," *IRE Transactions on Microwave Theory and Techniques*, Vol. 8, No. 5, 510–519, 1960.

[15] Gadhvi, D. D., S. K. Patel, and Y. Kosta, "Elliptic low pass filter design using DGS slot for microstrip lines," in *2013 Nirma University International Conference on Engineering (NUiCONE)*, 1–4, Ahmedabad, India, 2013.

[16] Vala, A., A. Patel, R. Goswami, and K. Mahant, "Defected ground structure based wideband microstrip low-pass filter for wireless communication," *Microwave and Optical Technology Letters*, Vol. 59, No. 5, 993–996, 2017.

[17] Soltani, S., H. Pakniat, and N. Yasrebi, "A wide stopband, high selectivity microstrip low-pass filter for wireless communications," *AEU — International Journal of Electronics and Communications*, Vol. 185, 155443, 2024.

[18] Jamshidi, M., A. Lalbakhsh, B. Mohamadzade, H. Siahkamari, and S. M. H. Mousavi, "A novel neural-based approach for design of microstrip filters," *AEU — International Journal of Electronics and Communications*, Vol. 110, 152847, 2019.

[19] Rekha, T. K., P. Abdulla, P. M. Jasmine, and A. R. Anu, "Compact microstrip lowpass filter with high harmonics suppression using defected structures," *AEU — International Journal of Electronics and Communications*, Vol. 115, 153032, 2020.

[20] Hong, J. S. G. and M. J. Lancaster, *Microstrip Filters for RF/Microwave Applications*, Wiley-Interscience, New York, 2001.